

REMARKS

Claims 1 and 4-15 are all the claims pending in the application.

I. Response to Rejection Under 35 U.S.C. 103

In the Office Action dated August 24, 2006, claims 1 and 4-15 remain rejected under 35 U.S.C. 103 as being unpatentable over Toru et al ("JP '156") as evidenced by its machine assisted translation, in view of Aoai et al. The Examiner's basic position is that in her view the formation of the polymers of Toru et al with a polydispersity as close to 1.0 as possible is prima facie obvious in view of Aoai teaching the desire to improve heat resistance and image forming characteristics by doing so. In response, Applicants have pointed out that "pattern profile" as described in Aoai et al and "LER" and "line width stability in vacuo" in the present invention are completely different characteristics from each other, and it is not unusual that though "pattern profile" is good, "LER" and "line width stability in vacuo" are not good. Accordingly, Applicants submit their claims are patentable over the cited prior art as based on the unexpectedness of the found correlation.

The Examiner maintains her position because (1) Applicants have not addressed the part of the range of Aoai et al not encompassed by Applicants' claims and (2) Applicants have not presented evidence showing the relationship or lack of relationship between LER and pattern profile.

With respect to point (1) above, the Examiner seems to suggest Applicants need to test a polymer having a dispersion degree of 1.6. However, Applicants have compared their claims

BEST AVAILABLE COPY

with the closest prior art in the 1.132 Declaration filed February 3, 2006, and therefore, the proper comparison has been made. The polymers of the primary reference are the closest prior art, and they have been tested. The polymer apparently suggested by the Examiner does not exist within the Examples of the primary reference and thus is not taught by the prior art. The Examiner recognizes that the polymers of the secondary reference are further removed from the present invention.

With respect to point (2) above, Applicants submit herewith two references establishing that a relationship between pattern profile and LER where a good characteristic in one of them means a good characteristic in the other is not necessarily the case, that is, improvement in one of them would not be understood by the skilled artisan to relate to an improvement in the other. Reference 1 is Proc. Of SPIE Vol. 5039, 1086-1097 (2003); reference 2 is J. Vac. Sci. Technol. Vol. 1B, No. 6, Nov/Dec 2000 (3340-3343).

Reference 1 studies the correlation of the basicity of a quencher with resist performance. In its conclusion at page 1096, Reference 1 states that "And as quencher ability is higher, generally, the profile is more vertical.... However, other lithographic properties such as LER and dark erosion were not affected by acid-quenching ability." Thus, Reference 1 clearly draws the conclusion that profile is a performance item not related to LER within the testing of the reference.

In Reference 2, the effect of changes in structure of photoacid generators (PAG) on resist imaging is studied. LER data are shown in Fig. 3(f), and data on pattern profile are shown in the right-hand side of Fig. 4 in the form of SEM photographs. While PAGs 2, 3 and 5 are excellent

with respect to LER as shown in Fig. 3(f), it is PAGs 1 and 4 that are excellent with respect to pattern profile as shown in Fig. 4, right-hand side. Note with respect to Fig. 4, a rectangular shape is most desirable, as in the PAGs 1 and 4 (some resist remains at the space between the pattern lines). Accordingly, Reference 2 shows there is no correlation between good LER property and good pattern profile, within that reference.

From the above, Applicants have responded and overcome the points raised by the Examiner as supporting her position. All claims are patentable over the prior art. The skilled artisan, within the confines of the present invention, would not equate good pattern profile with good LER.

Further, the Examiner is also respectfully requested to review the line width stability *in vacuo* data set forth in the submitted Rule 132 Declaration. See Tables A and B at pages 5 and 8 of the Declaration. Although no change in line width when the sample is left *in vacuo* is ideal, in practice the line width changes after development due to various mechanisms occurring. The range shown in the Examples of the present invention (1.6 to 1.7 in Table B) is a practically allowable limit, and when the change exceeds that limit as shown in the prior art (Table A), performance is judged to be unacceptable. Patentability is also established by the line width stability *in vacuo* comparative data.

In view of the foregoing, Applicants respectfully submit that the present claims are not obvious over the cited references and thus the rejection should be withdrawn.

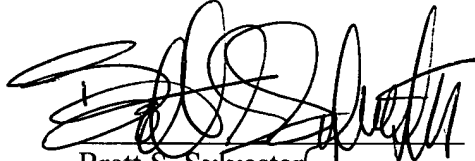
Response Under 37 C.F.R. § 1.111
U.S. Appln. No.: 10/812,092

II. Conclusion

Allowance is respectfully requested. If any points remain in issue which the Examiner feels may be best resolved through a personal or telephone interview, the Examiner is kindly requested to contact the undersigned at the telephone number listed below.

The USPTO is directed and authorized to charge all required fees, except for the Issue Fee and the Publication Fee, to Deposit Account No. 19-4880. Please also credit any overpayments to said Deposit Account.

Respectfully submitted,



Brett S. Sylvester
Registration No. 32,765

SUGHRUE MION, PLLC
Telephone: (202) 293-7060
Facsimile: (202) 293-7860

WASHINGTON OFFICE

23373

CUSTOMER NUMBER

Date: November 21, 2006

The Document 1



Effects of Quencher Ability on Profile in Chemically Amplified Resist System

Deogbae Kim, Hyun-Jin Kim, Sook-Hee Cho, Dong-Hwal Lee, Kwang-Hyi Im, Min-Ja Yoo, Sang-Hyang Lee, Jaehyun Kim (Electronic Materials Division 3, Dongjin Semichem Co., Ltd., 625-3, Yodang-Ri, Yanggam-Myun, Hwasung-Si, Kyungki-Do, South Korea, 445-930)
Jin-Soo Kim, Hyung-Soo Kim (Memory R&D Division, Hynix Semiconductor Inc., San 136-1, Ami-Ri, Ichon-Si, Kyungki-Do, South Korea, 467-701)

ABSTRACT

Recently, KrF lithography has extended to 100nm technical node using various techniques and pushed ArF lithography to sub-100nm application. To enhance resolution, there are many problems to be solved, like dark erosion (dark film loss), sloped profile, line edge roughness (LER), and so on. Also, thin resist film must be used to prevent pattern collapse. In general, the aspect ratio is less than 2.5 for sub 100nm. For this reason, chemically amplified resist has to get high etch resistance, low dark film loss and vertical profile shape at maximum resolution. Many efforts have been made to solve these problems and to improve resist performance. In this study, we tried to resolve some of these problems using various acid-quenching systems. We estimated the quencher ability using acid diffusion depth in resist film by sandwich method and pK_a value of amines. The changes of lithographic properties according to the application of different amines were investigated. It was found that acid-quenching ability of an amine was not related to its basicity from sandwich experiment results. In fact, quenching efficiency was more closely related to the amine molecular structure and bulkiness of a substituent attached to nitrogen atom. We observed that pattern shape and process margin were not directly related to the basicity of an amine, but more related to quenching efficiency. The amines having higher quenching ability show wider process margin. However, other lithographic properties such as LER and dark erosion were not affected by acid-quenching ability. It is believed that they are determined by other components including polymer, protection groups, and PAGs.

INTRODUCTION

Chemically amplified resists used in the manufacture of semiconductors, such as KrF resists and ArF resists, are comprised primarily of a partially blocked polymer(resin), photo-acid-generator(PAG), additives(acids-

quencher and surfactants), and solvents. Generally, it is well known that the optimization of amount of each component in resist solution is important in order to show good evaluation performance. And also the selection of each component is very important, because the relationship between the components affects the pattern profile, margins, photospeed, and etch selectivity. For example, in the selection of resin system, it appears that the narrow polydispersity of the resin will improve the photoresist performance.^{1,2} In early papers it was shown that the impact of photoacid generator structure and acid generation quantum efficiency were important factors for photolithographic performance.^{3,4} The addition of polymeric bases in resist system shows good performance.⁵

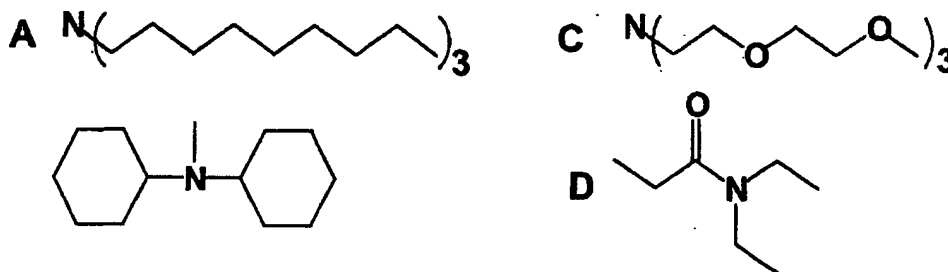
In this paper, we have checked that the quencher ability and its lithographic evaluation results to optimize resist performance in semiconductor manufacturing process.

EXPERIMENTAL

In this test, we used three kinds of polymer system, one is EE-PHS (partially ethoxyethyl blocked polyhydroxystyrene) to obtain quencher ability and another is blended polymer system to obtain KrF lithographic performance and the other is hybrid-COMA polymer for ArF lithographic performance. The blended polymer system for KrF and hybrid-COMA polymer were illustrated in our previous papers.⁶⁻⁸ And triphenylsulfonium perfluorobutanesulfonate ($C_4F_9SO_3H$) was added as PAG to resist to obtain litho performance.

The basicity of the quencher was measured using titration method. In this method, we used methanol/acetone=8/2 for solvent, 0.01N stock solution of perfluorobutanesulfonic acid ($C_4F_9SO_3H$) in methanol/acetone to titrate the amine solution and in the presence of methyl orange as an indicator.

We measured quencher ability ($c=a-b$) using sandwich method (Fig. 1).⁹ In this measurement, we selected four amines for quencher. The amine list is as follows;



Sandwich Method

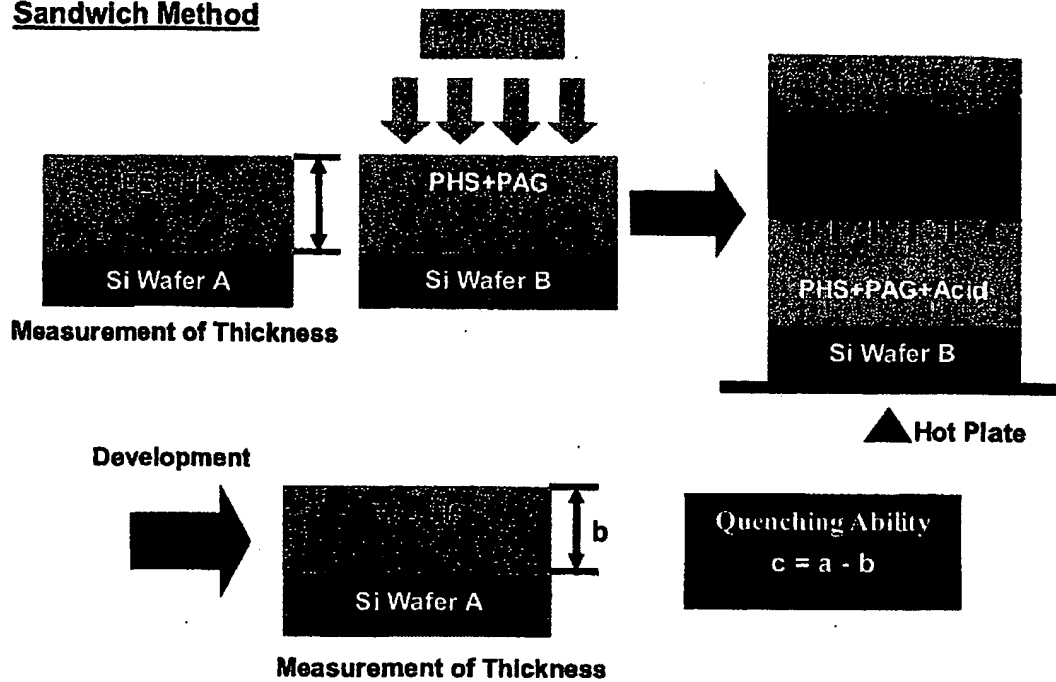


Fig. 1 Sandwich method to measure the acid-quenching ability.

We also used the sandwich method to measure the relative diffusion length of the generated acid.¹⁰ To obtain relative diffusion length, we coated top layer on a resin film. And relative diffusion length ($F=D-E$) was calculated from the thickness difference between reference film and residual film that included perfluorobutanesulfonic acid ($C_4F_9SO_3H$). (Fig. 2) The sequence is;

- (1) Preparation of solution
 - ✓ A : Resin + Amine
 - ✓ B : Top layer
 - ✓ C : Top layer + Acid ($C_4F_9SO_3H$)
- (2) Reference Film formation
 - ✓ Solution A coating (3000 Å → 110 °C/90s)
 - ✓ Solution B coating (3000rpm → 130 °C/10min)
 - ✓ Development (30sec in 2.38wt% TMAH Solution)
- (3) Measurement of Relative Diffusion Length
 - ✓ Solution A coating (3000 Å → 110 °C/90s)

- ✓ Solution C coating (3000rpm → 130°C/10min)
- ✓ Development (30sec in 2.38wt% TMAH Solution)
- ✓ Thickness measurement ; *Relative Diffusion length* ($F=D-E$)

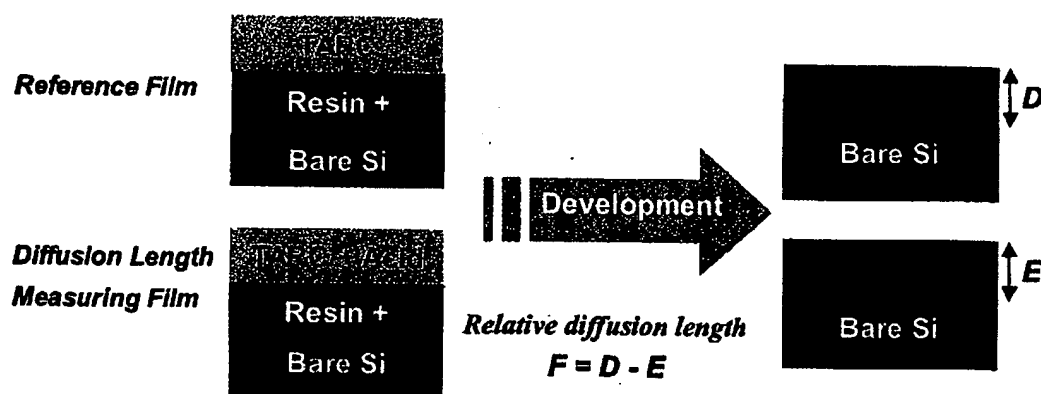


Fig. 2. Measurement of *Relative Diffusion Length* of the acid

RESULTS AND DISCUSSION

The basicity and quencher ability generally show a trade-off relation for various amines.(Fig. 3) We compared the pattern profile to the basicity and quencher ability of amines. (Fig 4) In this result, we found that the basicity of a quencher did not affect the pattern profile, meanwhile higher quencher ability showed better pattern shape.

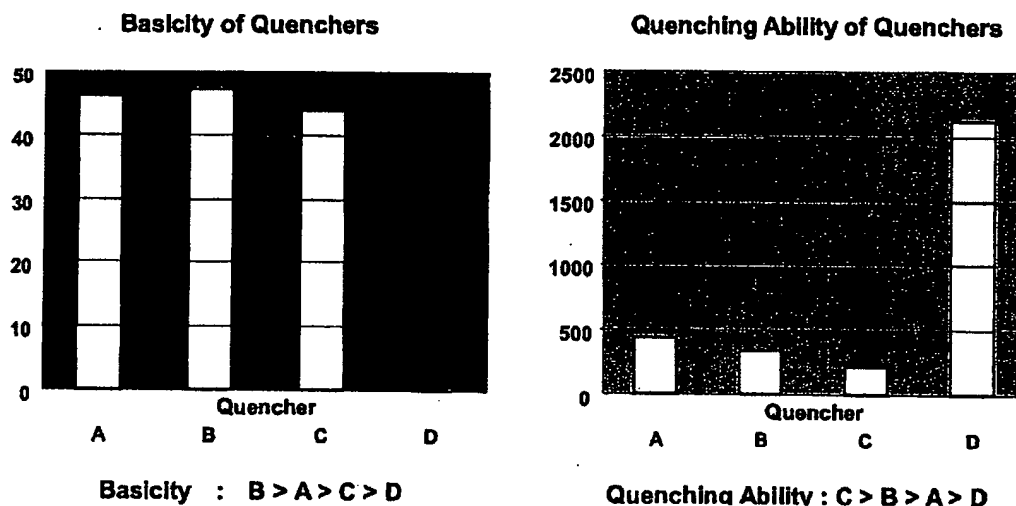


Fig. 4. Basicity and quencher ability of the amines

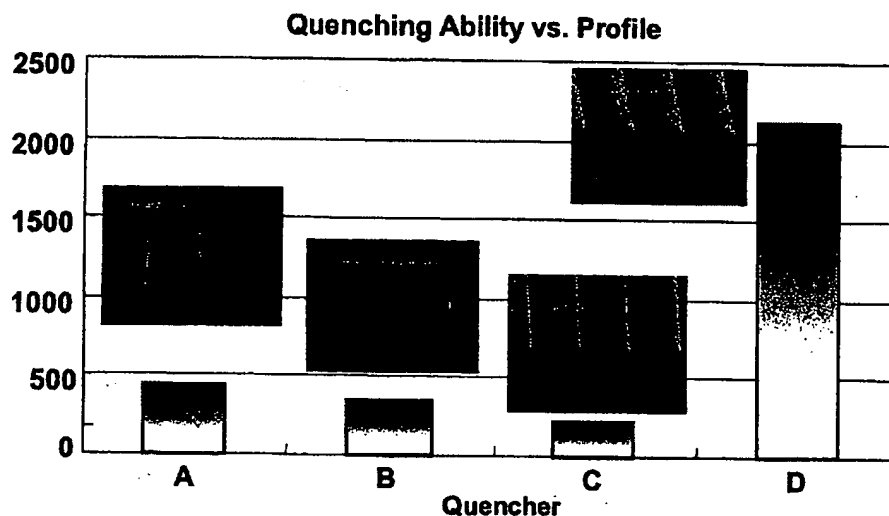


Fig. 5. Pattern profile with quencher abilities of the amines

We investigate the influence of relative acid diffusion length of the quenchers.(Fig 6) In this result, we realized that the quencher, including functional moiety like hydroxyl group or ketone group, showed shorter relative diffusion length. We think that the functional moiety supports to the ability of quencher by forming hydrogen bond, during the acid-base reaction.

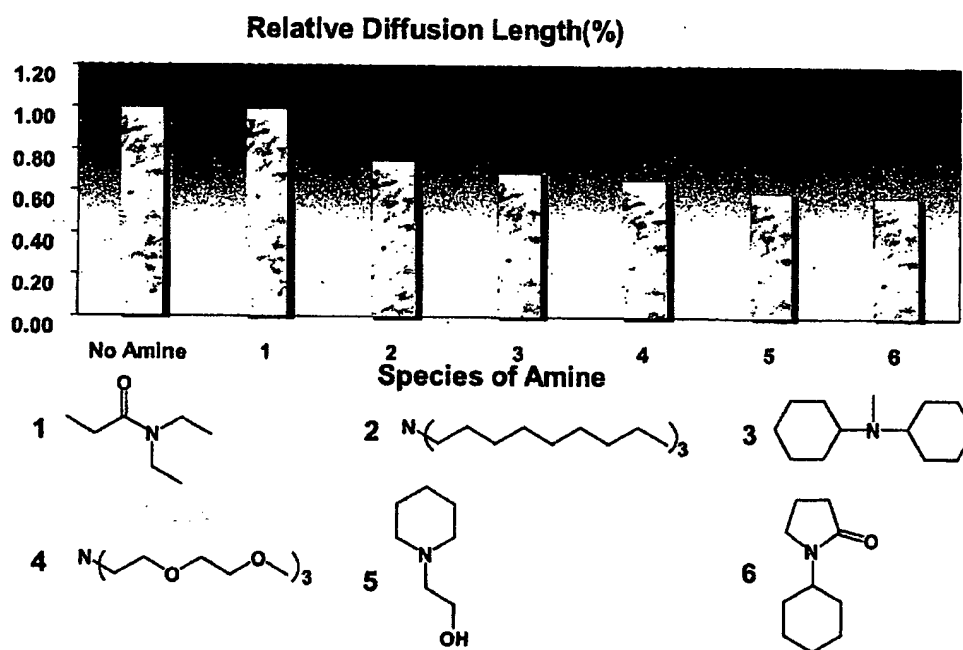


Fig. 6. Relative diffusion length of the quencher

We found that the pattern profile was influenced by acid diffusion length. The pattern shape of the resist that has shorter diffusion length by strong quencher shows more rectangular profile except 1.(Fig.7) The pattern shape of resist 1 shows T-topped profile, probably caused by low acid quenching efficiency.

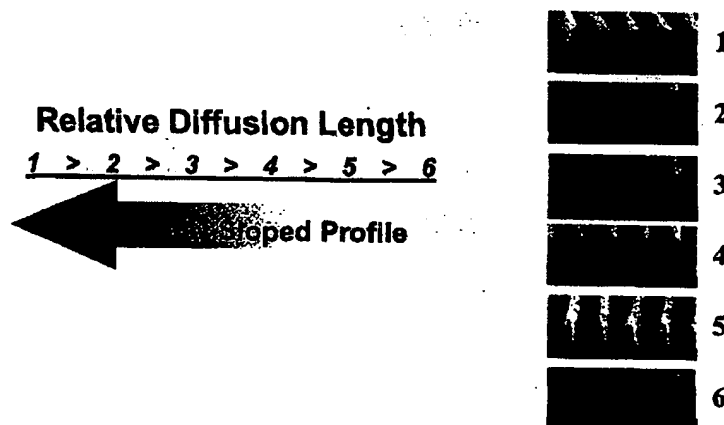
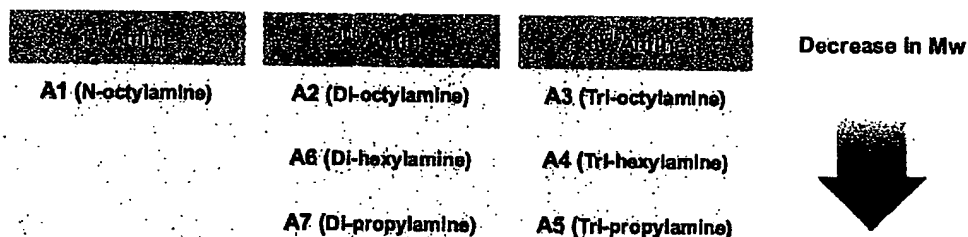


Fig. 7. Pattern profile related to acid diffusion length

We also obtained pattern profile using various quenchers, the result shows that the amine properties affected the acid quenching ability and pattern shape. In general, stronger quenching ability shows more vertical profile. (Fig. 8) This is the quencher list tested in this work;

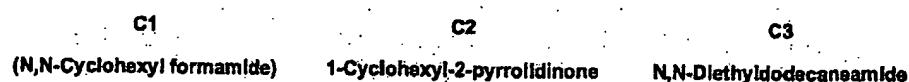
Group I (Aliphatic Amine)



Group II (Amine with side functional group)



Group III (Boiling point in amide amines)



Increase in Mw

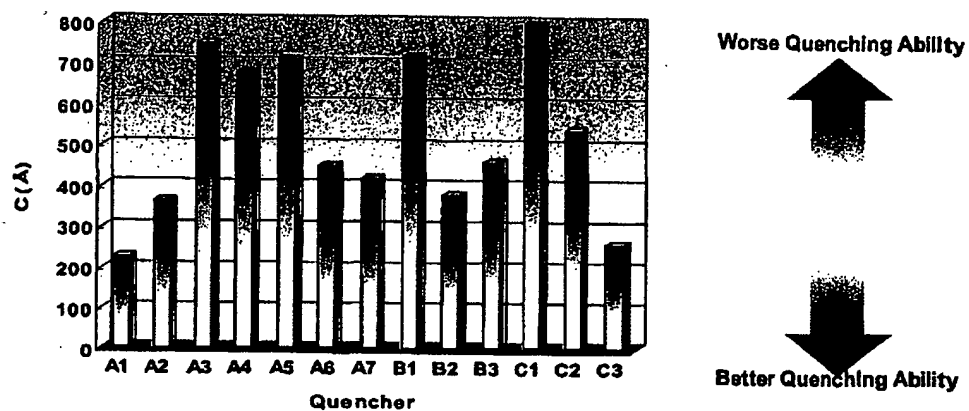



Fig. 8. Quencher ability according to amine

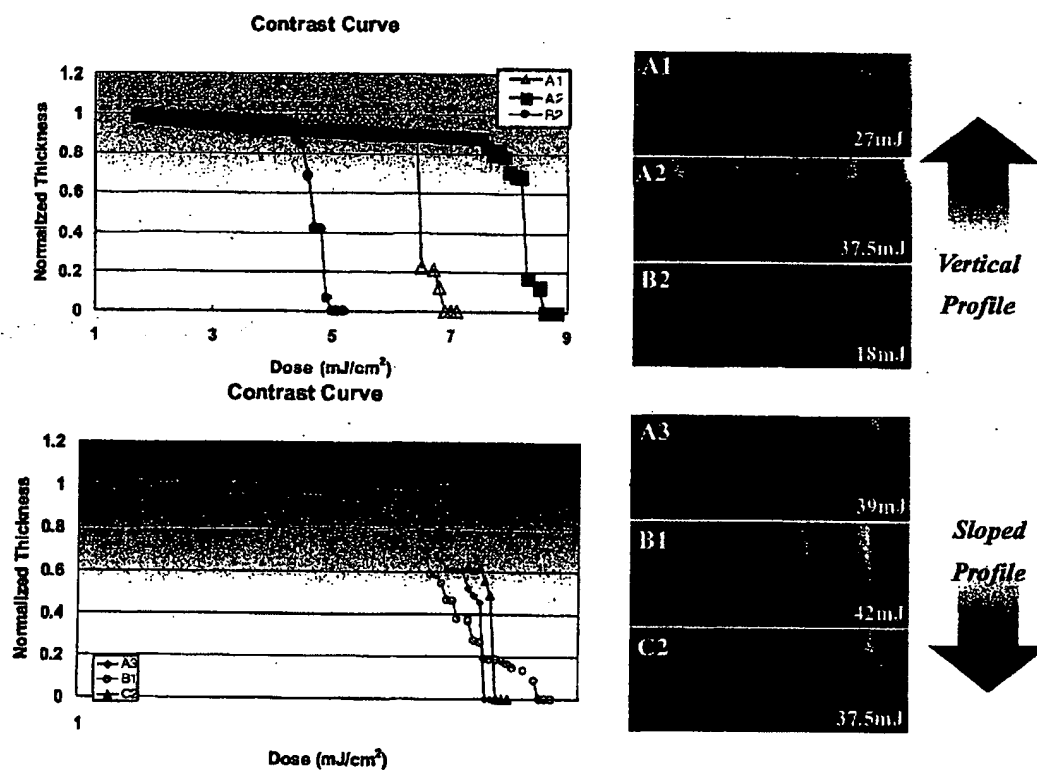


Fig. 9. Pattern profile change of the resist by using different quencher

In Figure 8, the quencher ability of primary amine was found to be better than secondary and tertiary amines.

But the molecular weight did not affect the quencher ability. And as boiling point of amine increased, the quenching ability was enhanced. Figure 9 clearly shows a relationship between quenching ability and pattern profile. These results suggest that the sloped profile can be corrected using an appropriate quencher that has high quenching ability. In Figure 10, there is no influence of molecular weight to pattern profile. But the boiling point of amines influenced to pattern profile (Fig. 11). The authors thought that lower boiling point amine will show T-shaped profile due to ease of amine evaporation during bake process. But the profile shape of low boiling point amine showed sloped profile instead of T-shaped. In contrast, the pattern slope was improved as the boiling point of the amine increased. It is probably due to higher concentration of residual amine in the resist film when high boiling point amine was employed. We will investigate this phenomenon to find the role of residual amine in resist in future.

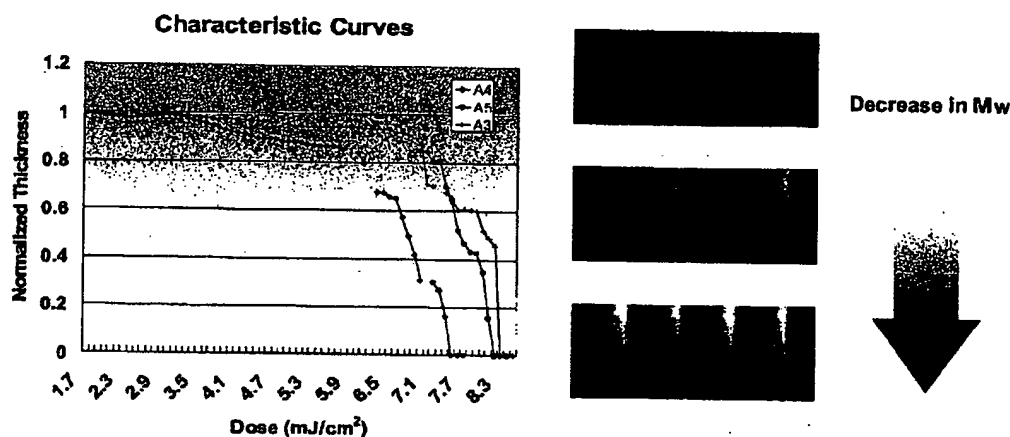


Fig. 10. Pattern profile related to quencher molecular weight

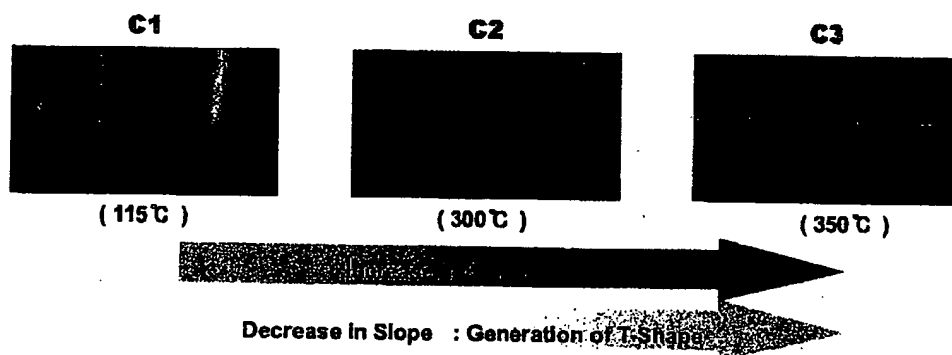
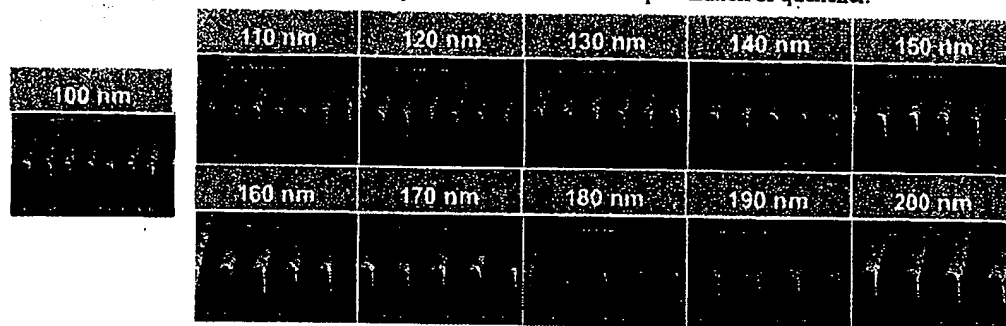


Fig. 11. Pattern profile due to boiling point of the quencher structure

After optimization of types and concentration of quenchers based on above results and careful selection of PAG and semi-protected polymer, we have obtained DUV resist system with good performance. Our new KrF

resist showed wide process margin even in 100nm 1:1 dense line and space pattern.(Fig. 12, 13, 14) The KrF resist also shows outstanding CD linearity from 200nm to 100nm still while it maintains DOF margins with ~400nm.

Fig. 12. CD Linearity of new KrF resist after optimization of quencher.



Process conditions

Substrate : Organic BARC

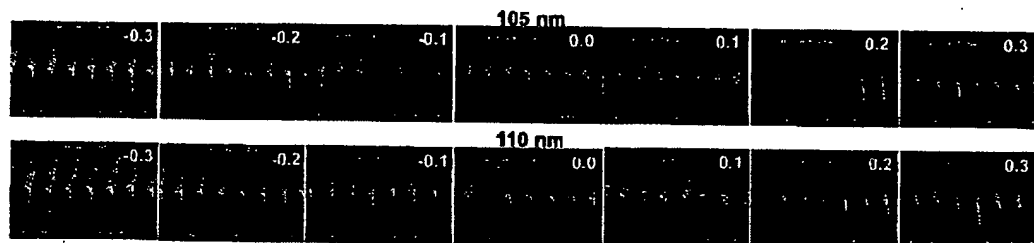
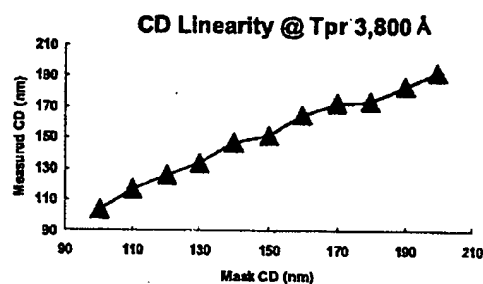
SOB : 100 °C/90sec

Exposure : NA 0.80

PEB : 100 °C/90sec

HB : 110 °C/75sec

Development : 2.38wt% TMAH



Process conditions

Substrate : Organic BARC

SOB : 100 °C/90sec

Exposure : NA 0.80

PEB : 100 °C/90sec

HB : 110 °C/75sec

Development : 2.38wt% TMAH

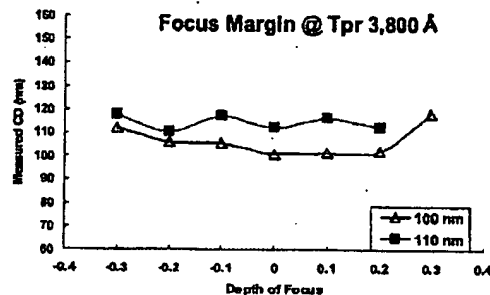


Fig. 13. Depth of focus margin of new KrF resist after optimization

For Isolate layer @ Target CD 100nm

Defocus (μm)	380	400	420	440	460	480
-0.4						
-0.3						
-0.2						
-0.1						
0						
0.1						
0.2						

CE	380	400	420	440	460	480	500
-0.4		8	80	79			
-0.3		112	93	67	68		
-0.2		118	95	95	70		
-0.1	8	127	99	94	87	70	61
0		8	108	85	77	75	
0.1		8	107	90	67		
0.2			109	63			
0.3			100				

Process conditions

Tpr : 2,700 Å

Substrate : Organic BARC

SOB : 100°C/90sec

Exposure : NA 0.80 (Cross pole)

PEB : 110°C/90sec

HB : 110°C/75sec

Development : 2.38wt% TMAH

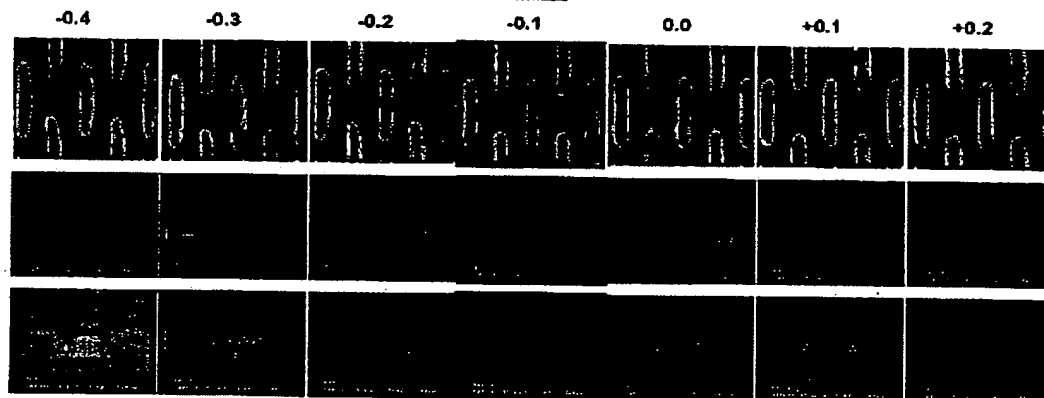


Fig. 14. Litho performance of new KrF resist for isolated pattern

In case of ArF resist system, after selection and optimization of new quencher system from this work, we obtained good pattern profile with no tailing and vertical shape.(Fig. 15)

Resist : ArF Hybrid Type (DHA-Series)

Exposure : ISI Stepper, NA 0.60 (6% PSM)

Tpr : 2,700Å (Organic BARC: DARC-A40)

SOB : 130°C/90sec, PEB : 130°C/90sec,

Target CD : 120nm

Development : 2.38wt% TMAH, HB : 110°C/60sec

Reference

Sample I

Sample II

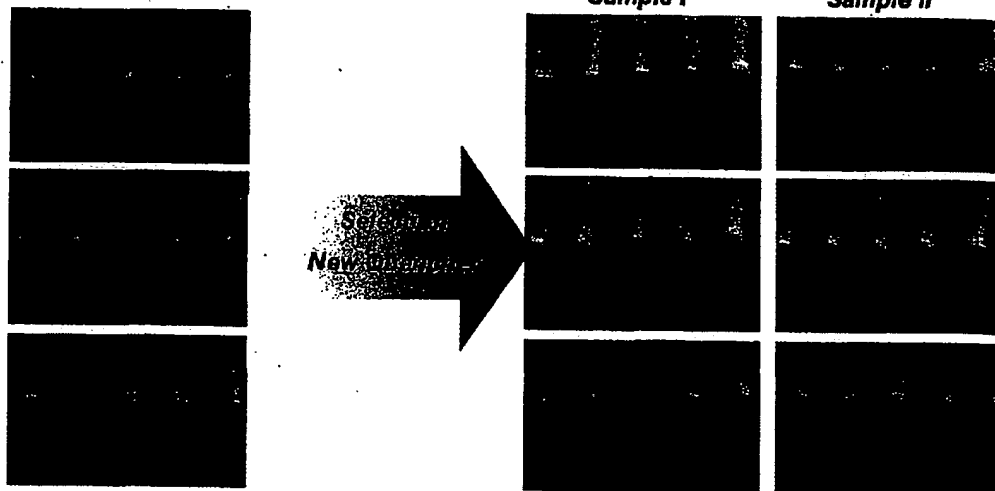


Fig. 15. Pattern profile of ArF after optimization of each component

CONCLUSION

We obtained that the acid quenching ability is different to their basicity. And as quencher ability is higher, generally, the profile is more vertical. As molecular weight of quencher increase, the quenching ability is almost same, thus the profile is not changed. As boiling point of quencher increase, the quenching ability increase, thus the slope of profile is improved. From the results, we realized that the pattern shape and process margin were not related to the basicity, but slightly related to the quenching efficiency in resist matrix. The Authors find that resist performance related to their components, and the optimization and selection of components can be the main factor in resist chemistry. From this research, we found that the amines having higher quenching ability showed wider process margin. However, other lithographic properties such as LER and dark erosion were not affected by acid-quenching ability. It is believed that they are determined by other components including polymer, protection groups, and PAGs. The relationship between LER and dark erosion and other components is being investigated and will be reported later.

ACKNOWLEDGMENTS

Authors would like to thank K. K. Kong for support of the resist development program and Y. S. Kim, H. L. Seo, and Y. D. Kim for corporations for resist evaluation in Memory R & D Division, Hyundai Electronics Industries Co. Ltd.

REFERENCE

1. M. Hanabata, F. Oi, and A. Furtua, *Poly. Eng. Sci.*, **32**, 1494(1992).
M. Hanabata, Y. Uetani and A. Furtua, *Proc. SPIE* **920**, 349(1988).
2. M.M. Cook, M. Dalil Rahman and P.H. Lu, *Proc. SPIE* **3333**, 1180(1998).
3. James F. Cameron, Sheri L. Ablaza, Guangyu Xu and Wang Yueh, , *Proc. SPIE* **3678**, 785(1999).
4. Charles R. Szmanda, Robert Kavanagh, John Bohland, James Cameron, Peter Trefonas and Robert Blacksmith, *Proc. SPIE* **3678**, 857(1999).
5. Wu-Song Huang, *Proc. SPIE* **3678**, 1040(1999)
6. S.J. Choi, Y.J. Choi, Y.S. Kim, S.D. Kim, D. Kim, and J. Kim, C.W. Koh, G. Lee., J.C. Jung and K.H. Baik, *Proc. SPIE* **4345**, 94 (2001)
7. Hyun-Jin Kim, Yoon-Sik Chung, Y-Jun Choi, Yang-Sook Kim, and Deogbae Kim, *Proc. SPIE* **4345**, 528 (2001)
8. Hyun-Jin Kim, Yoon-Sik Chung, Dong-Hwal Lee, Sook-Hee Cho, Kwang-Hwyi Im, Yoon -Gil Yim, Deogbae Kim, and Jaehyun Kim, *Proc. SPIE* **4690**, 651 (2002)
9. Eishi Shiobara, Daisuke Kawamura, Kentaro Matsunaga and Yasunobu Onishi,, *Proc. SPIE* **4345**, 628 (2001)
10. Jin-Baek Kim, Jong-Jin Park, Ji-Hyun Jang and Jae-Young Kim, *Proc. SPIE* **3678**, 625 (1999).

The Document 2

Modeling influence of structural changes in photoacid generators on 193 nm single layer resist imaging*

Ebo Croffie,^{a)} Lei Yuan, Mosong Cheng, and Andrew Neureuther
*Electronics Research Laboratory, The University of California at Berkeley, 211-19 Cory Hall,
 No. 1772, Berkeley, California 94720*

Frank Houlihan, Ray Cirelli, Pat Watson, and Om Nalamasu
Bell Laboratories, Lucent Technologies, 600 Mountain Avenue, Murray Hill, New Jersey 07974

Allen Gabor
Olin Microelectronics Materials, Inc., 200 Massasoit Avenue, East Providence, Rhode Island 02914

(Received 1 June 2000; accepted 11 September 2000)

We present recent modeling work aimed at understanding the influence of structural changes in photoacid generators (PAGs) on acid generation efficiency, deprotection efficiency, and photoacid diffusion in 193 nm chemically amplified resists. An analytical model for the postexposure bake process is used to study the reaction and diffusion properties of the various acids generated by the PAGs. Fourier transfer infrared spectroscopy is used to monitor the generation of photoacid during exposure. Resist thickness loss after PEB as a function of exposure dose is related to the deprotection extent to extract the reaction rate parameters. The effects of the acid size and boiling point on process latitude, line end shortening, and line edge roughness are presented. Analytical model predictions of process latitude and line end shortening are also presented and compared to experimental data. In this study, the photogenerated acid with the smallest molar volume and highest boiling point temperature gave the best overall lithographic performance. © 2000 American Vacuum Society. [S0734-211X(00)16606-5]

I. INTRODUCTION

The relative impact of acid diffusion and line-edge roughness effects on small feature reproduction in 193 nm chemically amplified resists (CAR) demands that factors influencing the pattern formation be investigated and controlled to allow extension of CAR for deep submicron resist applications. A cost effective way of investigating factors controlling pattern formation is through modeling and simulation.

Several studies of the role of photoacid generators (PAGs) on resist performance are available in the literature. Houlihan *et al.* studied the performance of photogenerators of sulfamic acids in chemically amplified single layer resists.¹ Allen *et al.*² studied the effects of structural changes in triflic acid generators on the performance of 193 nm resists.

We investigate the effects of onium salts of perfluorinate sulfonic acids on the lithographic properties of 193 nm single layer resists. A study of the surface composition of a norbornene/maleic anhydride based 193 nm photoresist for this class of PAGs suggest that the acid mobility depends on both the boiling point and the molar volume of the acid.³ The acid size and mobility impact the deprotection efficiency, acid diffusion, and line edge profile quality. We are interested in the impact associated with mobility and boiling point on the lithographic performance of 193 nm resists formulated with these PAGs.

*No proof corrections received from author prior to publication.

^{a)}Author to whom correspondence should be addressed; electronic mail: ebo@argon.eecs.berkeley.edu

II. RESIST CHEMISTRY

The PAGs used in this study include bis(*t*-butylphenyl)iodonium perfluoro-octanesulfonate (PAG 1), bis(*t*-butylphenyl)iodonium perfluorobenzenesulfonate (PAG 2), bis(*t*-butylphenyl)iodonium nonaflate (PAG 3), tris(*t*-butylphenyl)sulfonium nonaflate (PAG 4), and bis(α -ethoxycarbonyl-2,6-dinitrobenzyl) 1,3-benzenedisulfonate (PAG 5). The PAG structures are shown in Fig. 1(a). These PAGs were incorporated in 193 nm test resists with cycloolefinmaleic anhydride copolymers, cholate based dissolution inhibitor and a base quencher.⁴ PAGs 1, 2, and 3 have the same chromophore and are expected to have the same quantum yield. PAGs 3 and 4 produce the same acid. The acids that are generated from these PAGs differ in molar volume and boiling point⁵ as shown in Figs. 1(b) and 1(c), respectively. These different acids allow us to study the influence of the acid size and boiling point on fine feature lithography.

III. EXPERIMENT

All samples were processed under the following conditions unless otherwise stated. Resist samples were spun on HMDS primed 8 in. inorganic ARC coated wafers at 2050 rpm for 30 s. The samples were then soft baked at 145 °C for 90 s. Exposures were carried out on an ISI ArF 0.60 NA, $\sigma=0.7$, small field catadioptric exposure system. After exposure, PEB was performed at 155 °C for 90 s. The wafers were puddle developed with OPD-262 for 24 s. All resist processes were performed on TEL Superclean Track ACT 8. Resist thickness was measured using a thermowave opti-

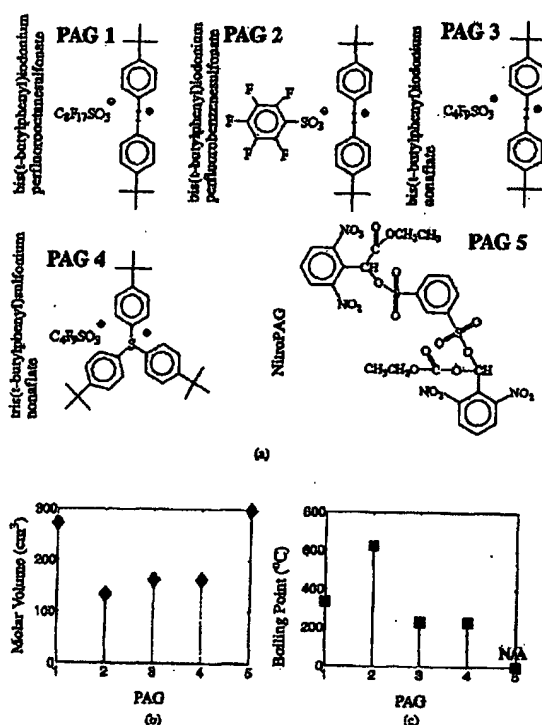


FIG. 1. (a) Photoacid generator structures; (b) molar volume of acid; (c) calculated boiling point (°C) corrected for triflic acid.

probe tool. Topdown scanning electron microscopy (SEM) micrographs and linewidth measurements were obtained using KLA Tencor 8100 CD SEM. All sample cross-section SEM micrographs were obtained using JEOL JSM 6400F scanning microscope except for PAG 2, which was obtained using LEO 1550 scanning microscope.

IV. POSTEXPOSURE BAKE ANALYTICAL MODEL

The following analytical expression for PEB is used in this study.

$$A(t) = 1 - \exp(-k_p H t), \quad (1)$$

$$H(t) = C_1 \tanh(C_1 k_p t - C_2) + C_1, \quad (2)$$

$$B(t) = C_1 \tanh(C_1 k_p t - C_2) - C_1, \quad (3)$$

$$C_1 = \frac{H_0 - B_0}{2}, \quad (4)$$

$$C_2 = \tanh^{-1} \left(\frac{H_0 + B_0}{B_0 - H_0} \right), \quad (5)$$

$$\frac{dx}{dt} = \sqrt{k_p D_0 (1-A) (1-\omega) \exp[\omega(1-A)]}, \quad (\omega < 1). \quad (6)$$

A is the extent of deprotection, H is the acid concentration, B is the quencher concentration, and dx/dt is the linewidth

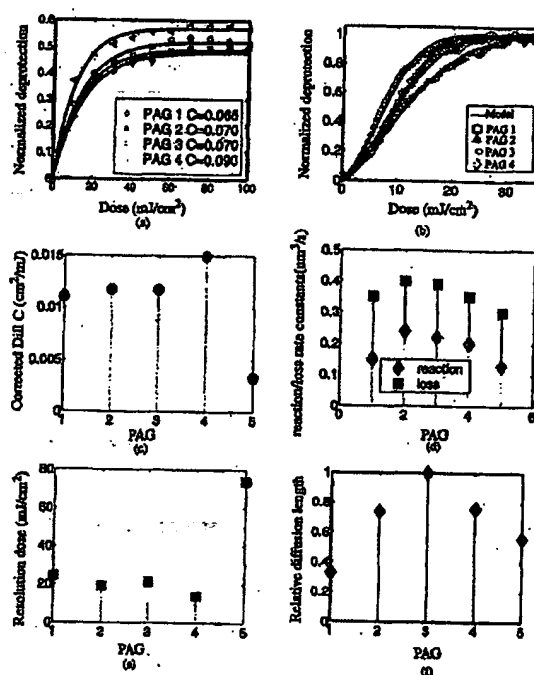


FIG. 2. (a) Extracting the Dill C parameter; (b) extracting reaction and acid loss rate parameters; (c) corrected C values, correction factor (1/6); (d) reaction and acid loss rate constants; (e) resolution dose; (f) relative diffusion length.

growth rate. D_0 and ω are diffusion parameters. The details of the model derivation are presented in Ref. 5.

V. PARAMETER EXTRACTIONS

A. Extraction of exposure parameters

The initial acid concentration (H_0) is needed to evaluate the above analytical model for PEB. This value is obtained using the Dill exposure model.⁶ To extract the Dill C parameter, we follow a method developed by Byers *et al.*⁷ The method rewrites Eq. (1) by substituting the acid generation equation for H , yielding the following expression:

$$A(t) = 1 - e^{-k_p (1 - e^{-C \text{Dose}}) t}. \quad (7)$$

We have assumed large dose exposures on antireflective coated substrates such that acid concentration changes with time during PEB is negligible. If we further assume low PEB temperature and time, Eq. (7) simplifies to the following:

$$A(t) = k_p t (1 - e^{-C \text{Dose}}). \quad (8)$$

Equation (8) allows the Dill C parameter to be extracted provided that the above conditions are met. To meet these conditions, the effect of acid diffusion on deprotection during PEB must be minimized. To minimize diffusion effects, organic ARC DUV 42-11 was spun on 8 in. wafers at 2740 rpm for 30 s. The ARC was baked at 200 °C for 60 s. Resist samples were prepared on the ARC coated wafers using the

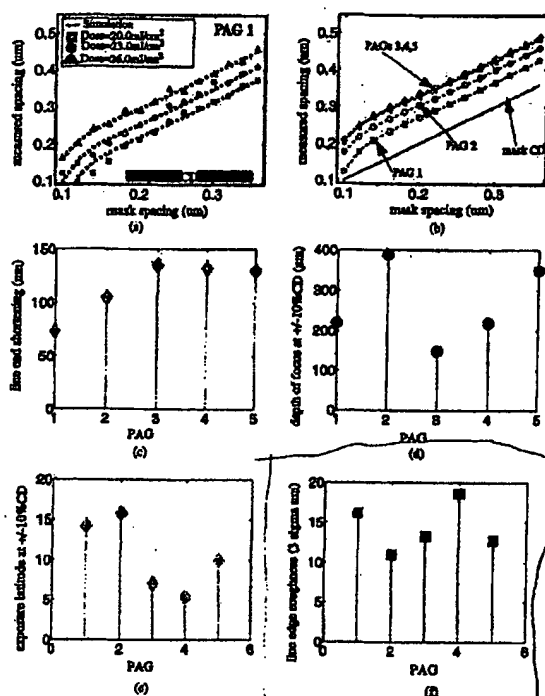


FIG. 3. (a) Model fitting of LES data to extract diffusion parameters; (b) comparing LES values for different PAG samples; (c) LES values; (d) depth of focus; (e) exposure latitude; (f) line edge roughness.

processing conditions and tools described above. Open frame exposures were carried out with doses ranging from 10 to 250 mJ/cm². Because of the small field size of the ISI stepper (1.5 mm×1.5 mm), 10×10 exposed fields were stitched together to provide a large enough exposed area for FTIR spectroscopy. From these large area open frame exposures, acid diffusion at the edges of the exposed region has negligible effects on the deprotection reaction. Furthermore, the ARC substrate minimizes standing waves such that the acid concentration vertical profile after exposure is close to uniform. From these conditions, it is reasonable to assume that diffusion effects are negligible during PEB.

The Nicolet MAGNA-IR 560 tool was used to monitor the deprotection reaction. The spectra were obtained in transmission mode. The decrease in absorbance near 1170 cm⁻¹ corresponds to the removal of *t*-butyl protecting groups.

Figure 2(a) shows the normalized deprotection extent (1138–1170 cm⁻¹) versus dose for PAGs 1–4. The samples were baked at 110°C for 45 s. The relative *C* values are obtained by fitting the deprotection versus dose data. The *C* values are corrected by a factor such that Eqs. (1)–(3) fit deprotection versus dose data for nominal PEB temperature and time. The correction factor used is (1/6). The corrected *C* values are plotted in Fig. 2(c). As expected, PAGs 1, 2, and 3 yield similar *C* values since they have the same chromophore.

TABLE I. Optimal model parameters.

	B_0	Dill <i>C</i>	k_r (μm ³ /s)	k_f (μm ³ /s)	ω	$A_{th}(\text{space})$	$A_{th}(\text{line})$
PAG 1	0.063	0.0110	0.15	0.35	0.9	0.30	0.41
PAG 2	0.090	0.0117	0.24	0.40	0.9	0.14	0.37
PAG 3	0.083	0.0117	0.22	0.39	0.9	0.20	0.50
PAG 4	0.079	0.0150	0.20	0.35	0.9	0.15	0.30
PAG 5	0.020	0.0033	0.13	0.30	0.9	0.36	0.60

B. Extraction of reaction rate parameters

To extract the reaction rate and acid loss rate constants, we relate resist thickness loss data after PEB to the extent of deprotection.⁸ The plots of normalized deprotection versus normalized resist thickness loss give unity slope. This allows us to use thickness loss after PEB data to extract the reaction and acid loss parameters. Figure 2(b) shows the normalized deprotection extent (from thickness loss data) as a function of exposure dose. The analytical model fit to this data yields the reaction rate constant and the acid loss constant. The reaction rate constant is related to the deprotection efficiency of the acid. Figure 2(d) shows that PAG 2 has the highest deprotection efficiency while PAG 5 has the lowest.

C. Extracting diffusion parameter

To characterize diffusion effects on image formation, line end shortening experiments were carried out using the processing conditions described above. The linewidth measurements for simulated profiles use a simple threshold model. This means resist which has deprotection extent higher than a given threshold, A_{th} , is considered to develop while resist below A_{th} is considered to remain. D_0 , ω , and A_{th} are tuned to determine the diffusivity parameters that best fit the LES measurements for different doses. Figure 3(a) shows the results of using the analytical model to fit LES data for PAG 1.

The relative diffusion length for the resolution dose of each PAG [Fig. 2(e)] as predicted by Eq. (6) for the above PEG conditions is plotted in Fig. 2(f). The acids generated from PAGs 3 and 4 show high diffusion length due to their small molar volume and low boiling point. The acid from PAG 1 with relatively large molar volume and higher boiling point shows the lowest diffusion length.

VI. RESULTS

A. Resolution

SEM micrographs of 130 nm dense features are shown in Fig. 3. It is seen that all the PAG samples are able to resolve 130 nm dense features except for the PAG 5 sample which shows more sidewall sloping and does not clear the resist to the substrate.

B. Model vs experiment comparison for process window and LES

The only drawback of the analytical model is that the optimum diffusion parameter (D_0) has to be obtained for different doses, necessitating a lookup table for D_0 as a

TABLE II. Comparing model prediction and experiment for process latitude.

	PAG 1	PAG 2	PAG 3	PAG 4	PAG 5
DOF (μm) from experiment	0.22	0.39	0.15	0.22	0.35
DOF (μm) from model	0.25	0.40	0.30	0.21	0.40
EL (%) from experiment	14.2	15.8	7.0	5.4	10.0
EL (%) from model	12.8	16.2	7.4	7.4	11.0

function of dose. Furthermore, the optimum D_0 values and threshold value (A_{th}) are different for lines (process window prediction) and spaces (line end shortening prediction). However this customization of D_0 and A_{th} to specific lithographic conditions allow the model to predict experimental data with high accuracy. The parameters used in the model prediction for process windows and line end shortening are summarized in Table I.

The process windows for 130 nm lines at $\pm 10\%$ CD from experiment and model equations are shown in Fig. 3. Table II compares the model prediction of the depth of focus (DOF) and exposure latitude (EL) to the experimental data. It is seen that the model prediction is consistent with experimental data. PAG 2 shows the largest process window because of its high deprotection efficiency and low diffusion

length. PAGs 3 and 4 show the smallest process windows due to their high diffusion lengths. Figures 4(d) and 4(e) plots the DOF and EL, respectively.

Figure 4(a) shows the line end shortening (LES) data and model fit for PAG 1 for different doses. Similar fits were done on PAG data for all test resists to obtain the diffusion parameters for the different samples. These parameters are used to predict the LER for the different PAG samples at their resolution doses. The results are plotted in Figs. 4(b) and the LES values are plotted in Fig. 4(c). It is seen that PAG 1 gives the lowest LES, followed by PAG 2. PAGs 3–5 give high LES values.

C. Line edge roughness

Line edge roughness (LER) analysis on the various PAG samples were performed using the graphically oriented resist analysis (GORA) software v. 1.65. The results of the analysis are plotted in Fig. 4(f). It is seen that the sample with PAG 2 gives the least LER.

VII. CONCLUSION

In this article, the influence of structural changes in PAGs on acid generation efficiency, deprotection efficiency and

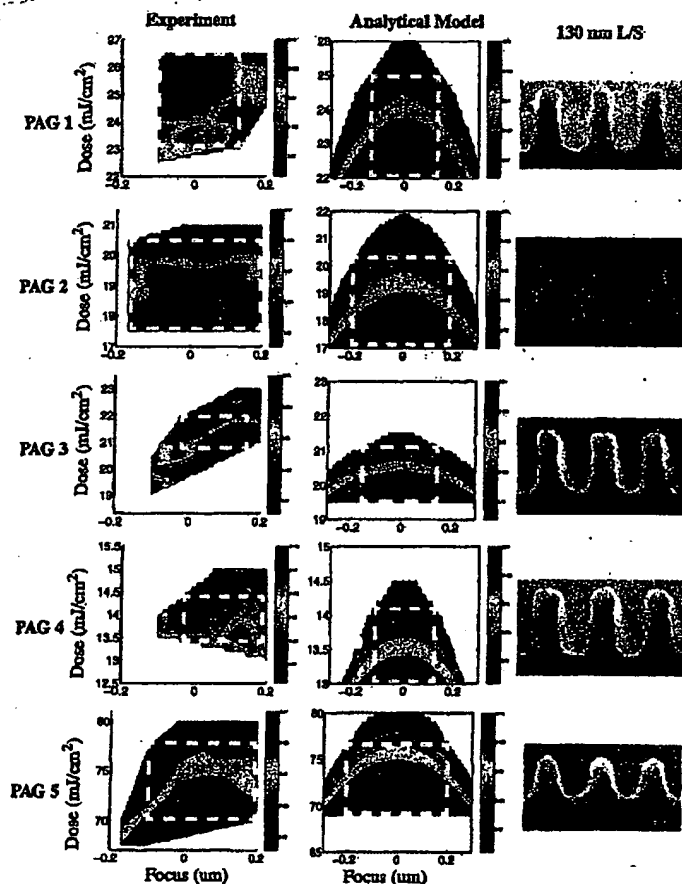


FIG. 4. Process windows for 130 nm lines at $\pm 10\%$. Experiment (left-hand side) and analytical model prediction (middle); 130 nm dense features (right-hand side).

photoacid diffusion, and their effects on line end shorting, process latitude and line edge roughness were documented. The acid size and boiling point influence the deprotection efficiency and acid diffusion and consequently the resist performance in fine feature lithography. An analytical model for the postexposure bake process was used to quantify the deprotection efficiency and the diffusion length and their effects on line end shortening and process latitude. It was found that PAG 2 gave the best overall performance in terms of having a low resolution dose (for throughput considerations), the highest deprotection efficiency, relatively low diffusion length and line end shortening effect, the largest process window, and the lowest line edge roughness. These good performance of PAG 2 resists sample is attributed to the small acid size and high boiling point temperature.

ACKNOWLEDGMENTS

The authors would like to thank Kevin Bolan, Gary Forsythe, and Carol Lochstamphoe (Bell Laboratories) and Kim

Chan (UC Berkeley Electronic Research Laboratories) for their help in collecting the experimental data. This research was jointly sponsored in part under SRC Contract No. 96-LC-460 and DARPA Grant No. MDA972-97-1-0010.

¹F. M. Houlihan, J. M. Kometani, A. G. Timko, R. S. Hutton, R. A. Cirelli, E. Reichmanis, O. Nalamasu, A. H. Gabor, A. N. Medina, J. J. Biafore, and S. G. Slater, *J. Photopolym. Sci. Technol.* 11 (1998).

²R. D. Allen, J. Opitz, C. E. Larson, R. A. DiPietro, G. Breyta, and D. C. Hofer, *Proc. SPIE* 3049, 44 (1997).

³H. W. Krautter, F. M. Houlihan, R. S. Hutton, I. I. Rushkin, and R. L. Opila, *Proc. SPIE* 3999 (2000).

⁴F. M. Houlihan, T. Wallow, A. Timko, E. Neria, R. Hutton, R. Cirelli, J. M. Kometani, O. Nalamasu, and E. Reichmanis, *J. Photopolym. Sci. Technol.* 10 (1997).

⁵E. Croffie, M. Cheng, A. Neureuther, F. M. Houlihan, R. A. Cirelli, J. Sweeney, G. Dabbah, O. Nalamasu, I. Rushkin, O. Dimov, and A. H. Gabor, *Proc. SPIE* 3999 (2000).

⁶F. Dill, A. Neureuther, J. Tuttle, and E. Walker, *IEEE Trans. Electron Devices* ED-22, 456 (1975).

⁷J. Byers (private communication).

⁸A. H. Gabor, L. C. Pruett, and C. K. Ober, *Chem. Mater.* 8, 2282 (1996).

**This Page is Inserted by IFW Indexing and Scanning
Operations and is not part of the Official Record**

BEST AVAILABLE IMAGES

Defective images within this document are accurate representations of the original documents submitted by the applicant.

Defects in the images include but are not limited to the items checked:

- ☐ BLACK BORDERS
- ☒ IMAGE CUT OFF AT TOP, BOTTOM OR SIDES
- ☒ FADED TEXT OR DRAWING
- ☐ BLURRED OR ILLEGIBLE TEXT OR DRAWING
- ☐ SKEWED/SLANTED IMAGES
- ☐ COLOR OR BLACK AND WHITE PHOTOGRAPHS
- ☐ GRAY SCALE DOCUMENTS
- ☒ LINES OR MARKS ON ORIGINAL DOCUMENT
- ☐ REFERENCE(S) OR EXHIBIT(S) SUBMITTED ARE POOR QUALITY
- ☐ OTHER: _____

IMAGES ARE BEST AVAILABLE COPY.

As rescanning these documents will not correct the image problems checked, please do not report these problems to the IFW Image Problem Mailbox.